공학석사 학위논문

Mechanism of Synthesizing Sulfur-Rich Polymer Nanoparticles and Their Surface Modification

고 황 함유 고분자 나노 입자 합성의 메커니즘 및 표면 개질

2017년 8월

서울대학교 대학원

화학생물공학부

박 정 민

Abstract

Recent surge of global energy consumption causes a sharp increase in sulfur production as it is produced as a byproduct of natural gas and oil refining operations. With sulfur and sulfur-containing materials exhibiting an array of desirable properties ranging from high electrochemical capacities to high refractive indices, methods of directly utilizing cheap and abundant sulfur for advanced materials is of great interest. One major hurdle against achieving such useful materials from elemental sulfur is the low solubility in common solvents. In order to fully exploit the desirable properties of elemental sulfur, methods to prepare high sulfur-content materials in processible form are crucial.

We herein report the synthesis mechanism and surface modification of sulfur-rich polymer nanoparticles (NPs) from interfacial polymerization of sodium polysulfide and 1, 2, 3-trichloropropane in water. Among three types of surfactants (anionic, neutral, and cationic), well-defined spherical shape NPs are obtained only in case of cationic surfactant. This is because only cationic surfactant can transfer the anionic polysulfide into

micelle (role of Phase Transfer Catalyst). Synthesizing NPs by using neutral surfactants and PTC, proposed mechanism can be proved in indirect way.

The surface of polysulfide nanoparticles could be functionalized first by using end-modified surfactants followed by the UV induced radical addition reaction. The method allows for the preparation of stable polysulfide nanoparticles with positively charged surfaces.

Keywords: sulfur, polysulfide polymer, interfacial polymerization, polymer nanoparticles, mechanism, phase transfer catalyst, surface modification

Student number: 2015-21065

Contents

List of Tables

List of Figures

Ⅰ. Introduction

Recent rapid rise in global energy consumption is also causing a sharp increase in sulfur production (about seven million tons annually) as it is produced as the byproduct of natural gas and oil refining operations. [1, 2]

Sulfur and sulfur-containing materials exhibiting an array of desirable properties ranging from nontoxic pesticide to high IR transparency.

Traditionally it is known that sulfur-containing compounds have nontoxic pesticidal properties in agriculture [3]. Elemental sulfur has high storage capacity per weight for alkaline metals that can be directly used in cathodes for secondary batteries from lithium-sulfur batteries [4] to sodium-sulfur batteries [5]. In high refractive index polymer materials, sulfur is the most promising atom for increasing refractive index due to its high atomic polarizability and good stability [6]. Sulfur-rich materials also have potential for IR optical applications because of high IR transparency [7]. Although it has many desirable properties, there are some limitations in application until now. Among them, one major obstacle towards achieving such useful materials from elemental sulfur is the

low solubility in common solvents of sulfur-rich materials [8, 9]. In order to fully exploit the desirable properties of elemental sulfur, several methods of directly utilizing the cheap and abundant sulfur in the synthesis of advanced materials is of great interest.

One of well-known methods is using polysulfide anion. Polysulfide anions can be formed by dissolution of elemental sulfur in basic solution including sodium sulfide aqueous solution [10]. In polysulfide anions, as the form of S_n^{2-}, n is the average sulfur atoms per anion and it can be controlled. Synthesis procedure and various structure of various rank of polysulfide was already studied [11].

To exploit these reduced sulfur species into polymeric materials, various organic halide monomers were used as comonomers. Polymerization occurs at the interface of aqueous polysulfide and organic halide phase due to mutual immiscibility. The first polysulfide polymer using interfacial polycondensation was synthesized from ethylene dichloride and potassium polysulfide by German chemists C. Lowig and S. Weidmann in 1840[12]. Various organic dichloro- or dibromo- monomers were investigated as backbone structure to enhance the yield and mechanical properties in the presence of cationic surfactant accelerating interfacial polymerization [13, 14]. Cationic surfactant do role as a phase

transfer catalyst (PTC) which promotes reactions even in mild conditions with environmentally benign reactants and solvents. With phase transfer catalyst, typically formation of polymers through interfacial polycondensation can be promoted [15-21].

Instead of organic dihalide monomers, a small amount of 1,2,3-trichloropropnae (TCP) is used to introduce branched structures in the polysulfide polymer chains. Resulting cross-linked polymer has both high yield and extremely high chemical resistance, which can be used in several applications mentioned above. On the other hand, high chemical resistance also means lack of solubility, which leads to low solution processability. It had its own limit in the form of polymer dispersion, thus difficult to carry out further processing of the polysulfide polymers [22]. To overcome this obstacle, polymers in nanoparticle form which are easily processable in dispersed state, can be used.

We herein report the synthesis of sulfur-rich polymer nanoparticles from interfacial polymerization of sodium polysulfide and 1,2,3-trichloropropane in water. Aqueous sodium polysulfide is prepared by dissolving elemental sulfur in sodium sulfide solutions. The treatment of the sodium polysulfide solution with 1,2,3-trichloropropane in the presence of suitable surfactants and phase-

transfer catalysts affords polycondensation products as well-defined nanoparticles. The obtained nanoparticles show well-defined spherical shape nanoparticles with narrow particle size distribution. Size of the nanoparticles can be controlled by rank of polysulfide, concentration of surfactant and chain length of surfactant. In addition, sulfur content of the polysulfide polymers are dependent on rank of the polysulfide anions. Cationic surfactant CTAB carries the anionic polysulfide to the TCP in organic phase, accelerating the formation of nanoparticle. It can be indirectly examined by replacing CTAB with non-ionic surfactant and Phase transfer catalyst, showing that CTAB has dual role as a surfactant and PTC. Instead of CTAB, new surfactant having terminal alkene is first used in the same synthesis procedure, followed by the UV induced radical addition reaction. This method allows for covalent bond between thiol on surface of the nanoparticle and terminal alkene bond in the surfactants. It helps to keep positively charged surface and have resistance for washing with water.

Ⅱ. Experimental Details

1. Materials

Elemental sulfur (from Samchun chemical, 99.5%), sodium sulfide (from Aldrich, nonhydrated), 1,2,3-trichloropropane (TCP, from Aldrich, 99 %), cetyltrimethylammonium bromide (CTAB, from Aldrich, 98 %), sodium dodecylammonium sulfate (SDS, from Aldrich, 99%), Triton x-100 (from Aldrich, average mol wt. 625), N-Bromosuccinimide (from Aldrich, 99%), potassium tert-butoxide,1.0M THF solution (from Aldrich, 99%), triphenylphosphine (from Fischer chemical, general purpose grade), trimethyl amine(from Aldrich, 31-35wt% in ethanol), dichloromethane (from Samchun chemical, 99.5%), and hexane (Samchun chemical, 95%) were used as received. Deionized water was degassed by nitrogen gas for at least 1 hour before use.

2. Synthesis of polysulfide polymer nanoparticles

All the polymerization procedures were conducted under nitrogen atmosphere after vacuum purging process using Schlenk technique. Sodium polysulfide stock solutions with various rank were prepared by dissolving elemental sulfur (321 mg for disulfide, 642 mg for

trisulfide, 963 mg for tetrasulfide and 1120 mg for rank 4.5 polysulfide) into solution of sodium sulfide (780 mg, 10 mmol) with 8 mL of degassed water in a septum-sealed 20 mL scintillation vial. After dissolving sulfur completely by stirring at 600 rpm, degassed water was added until the solution was 10 mL to prepare 1 M of sodium polysulfide solution.

To a 20 mL scintillation vial containing stirring bar maintained at 30 ^{0}C in a heating block, 9.9 mL of degassed water was added followed by addition of 100 μL (0.1 mmol of polysulfide) of polysulfide stock solution via microsyringe. Upon complete dissolution of sodium polysulfide into water, 0.2 mmol of phase transfer catalyst (72.9 mg of cetyltrimethylammonium bromide, 57.7 mg of sodium dodecylsulfate, 125 mg of triton x-100) was added while stirring and temperature at 30 ^{0}C until complete dissolution. Subsequently the solution was charged with 1,2,3-trichloropropane (21.3 μL for 0.2 mmol) via microsyringe. Initial pale yellow polysulfide solution turned to turbid white after 4 hours when the interfacial polycondensation reaction proceeded to result in nanoparticles.

3. Analysis of polysulfide polymer nanoparticles

After completion of reaction, 100 μL aliquot of reaction mixture was withdrawn from turbid white polymer nanoparticles dispersion and diluted into 9.9 mL of degassed water. The diluted solution was sonicated to be dispersed, and was used for dynamic light scattering (DLS) and zeta potential measurements (zetasizer Nano ZS90, Malvern).

Polysulfide polymer nanoparticles were purified from reaction mixture by centrifugation at 12000 rpm for 10 minutes followed by redispersion–centrifugation methods for 3 times. Then the washed nanoparticles was redispersed in degassed water and dropped on the silicon wafer followed by *in vacuo* drying and analyzed by scanning electron microscope (SEM; JSM-6701F, ZEOL). The washed nanoparticles were also analyzed by elemental analyzer (EA; Flash2000, Thermo Scientific).

4. Synthesis of trimethylpentadeceneammonium bromide (PTAB) and surface modification

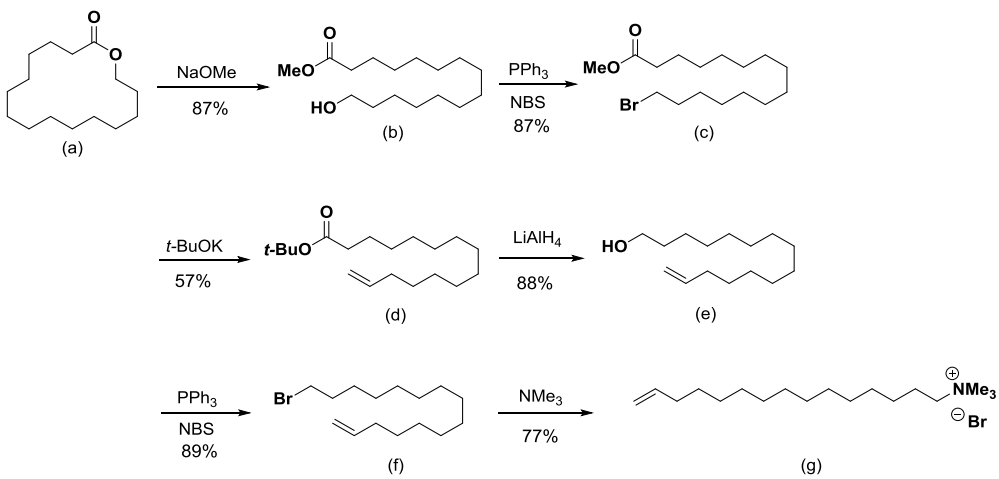

Figure 1. Synthetic procedure of trimethylpentadeceneammonium bromide (PTAB)

To prepare trimethylpentadeceneammonium bromide (PTAB), six steps of synthesis is conducted. All the polymerization procedures were conducted under nitrogen atmosphere after vacuum purging process.

Synthesis of methyl 15-hydroxypentadecanoate (b)

5.6g of sodium metal is added to 300ml of anhydrous methanol with ice bath. After the sodium metal fully disappeared, 12.1ml of w-pentadecalactone is added and react at 80℃ for 4hours. Quenching is achieved by 1M HCL solution, followed by diethyl ether extraction for three times. Column chromatography from hexane/ Ethyl acetate (2:1 by volume) separate the methyl 15-hydroxypentadecanoate (b) from impurities and the compounds were obtained as white solid. Yield is 87%.

Synthesis of methyl 15-bromopentadecanoate (c)

7.9g of methyl 15-hydroxypentadecanoate and 15.3g of triphenyl phosphine (PPh_3) is added to 55ml of anhydrous dimethylformamide (DMF). N-bromosuccinimide (NBS) is injected into mixture slowly by dropwise. Reaction goes for one hour at 55℃. 1M HCL and methanol is used to quench the reaction, followed by three times of extraction by diethyl ether. Hexane is used to dissolve the product and methyl 15-bromopentadecanoate (c) is obtained as a white solid by column chromatography (hexane/ethyl acetate = 20:1 by volume). Yield is 87%.

Synthesis of tert-butyl pentadec-14-enoate (d)

8,7g of methyl 15-bromopentadecanoate (c) is added to 125ml of potassium tert-butoxide (t-BuoK) in THF (1.0M), reacting at room temperature for one hour. Quenching is achieved by 1M HCL solution, followed by diethyl ether extraction for three times.

Tert-butyl pentadec-14-enoate (d) is obtained as a yellow liquid by column chromatography (hexane/dichloromethane = 5:1 by volume). Yield is 57%.

Synthesis of pentadec-14-en-1-ol (e)

6.35g of tert-butyl pentadec-14-enoate (d) is added to 16ml of Lithium aluminum hydride ($LiAlH_4$) in Ether (1.0M) dropwisely. Reaction is for 1 hour at 50℃. Quenching is achieved by dilute sulfuric acid, followed by diethyl ether extraction for three times.

Pentadec-14-en-1-ol (e) is obtained as a white solid by column chromatography (hexane/Ethyl acetate = 10:1 by volume). Yield is 88%.

Synthesis of 15-bromopentadec-1-ene (f)

4.3g of pentadec-14-en-1-ol (e) and 10g of triphenyl phosphine(PPh_3) is added to 35ml of dimethylformamide (DMF),followed by addition of 6.8g of N-bromosuccinimide(NBS) very slowly. Reaction takes for one hour at 55℃. Quenching is achieved by methanol and 1M of HCL, followed by diethyl ether extraction for three times. . Hexane is used to dissolve the product and 15-bromopentadec-1-ene (f) is obtained by column chromatography (hexane 100% by volume). Yield is 89%.

Synthesis of trimethylpentadeceneammonium bromide (g)

4.2g of 15-bromopentadec-1-ene (f) is added to 11.5ml of trimethylamine ethanolic solution (4.2M). Reaction goes for 48 hours at room temperature. Minimum quantities of DCM is used only to dissolve the product, followed by addition of hexane (1.5 times of DCM) to make the precipitation. Then, filtering is conducted and recrystallization by ether/ethanol (8:2 by volume) yield only pure final product. Yield is 77%

The synthesized surfactant, PTAB, was used for surface modification of polysulfide polymer nanoparticles through covalent bond on the surface. Instead of CTAB, PTAB is used to previously

synthesis procedure of polymer nanoparticles. Then 250nm of UV is radiated to the nanoparticles, resulting in well-dispersed nanoparticles with positive charge on the surface.

Ⅲ. Results and Discussion

1. Synthesis of Sulfur-Rich NPs through Interfacial Polymerization

Sulfur-Rich NPs could be synthesized by interfacial emulsion polymerization by following very simple synthesis procedure (Figure 2). Under nitrogen atmosphere, TCP reacts with prepared aqueous polysulfide, resulting in well-defined spherical shaped sulfur-rich nanoparticles, which could be proved by SEM images and DLS analysis (Figure 3).

Completion of interfacial polycondensation between polysulfide and TCP was determined by detection of fading away of color of polysulfide and the detection of turbidity according to the formation of nanoparticles, which causes scattering of the visible light. Within 4 hours, the solution of reactant mixture turned to turbid milky and before analysis, it was held for further 12 hours. The characteristic yellow color of polysulfide solution disappeared as the interfacial polymerization is proceeded with TCP under dilute condition (10×10^{-3} M) with surfactant (20×10^{-3} M) and vigorous stirring at 30 ^{0}C.

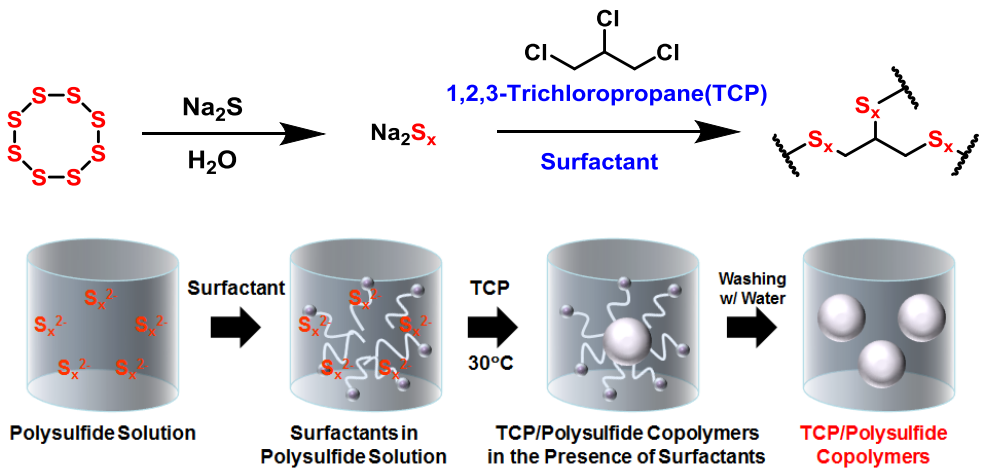

Figure 2. Synthetic procedure of polysulfide polymer from sodium trisulfide and 1,2,3-trichloropropane (TCP) in the presence of surfactant (top), and illustration of NP synthesis followed by purification by washing with water.

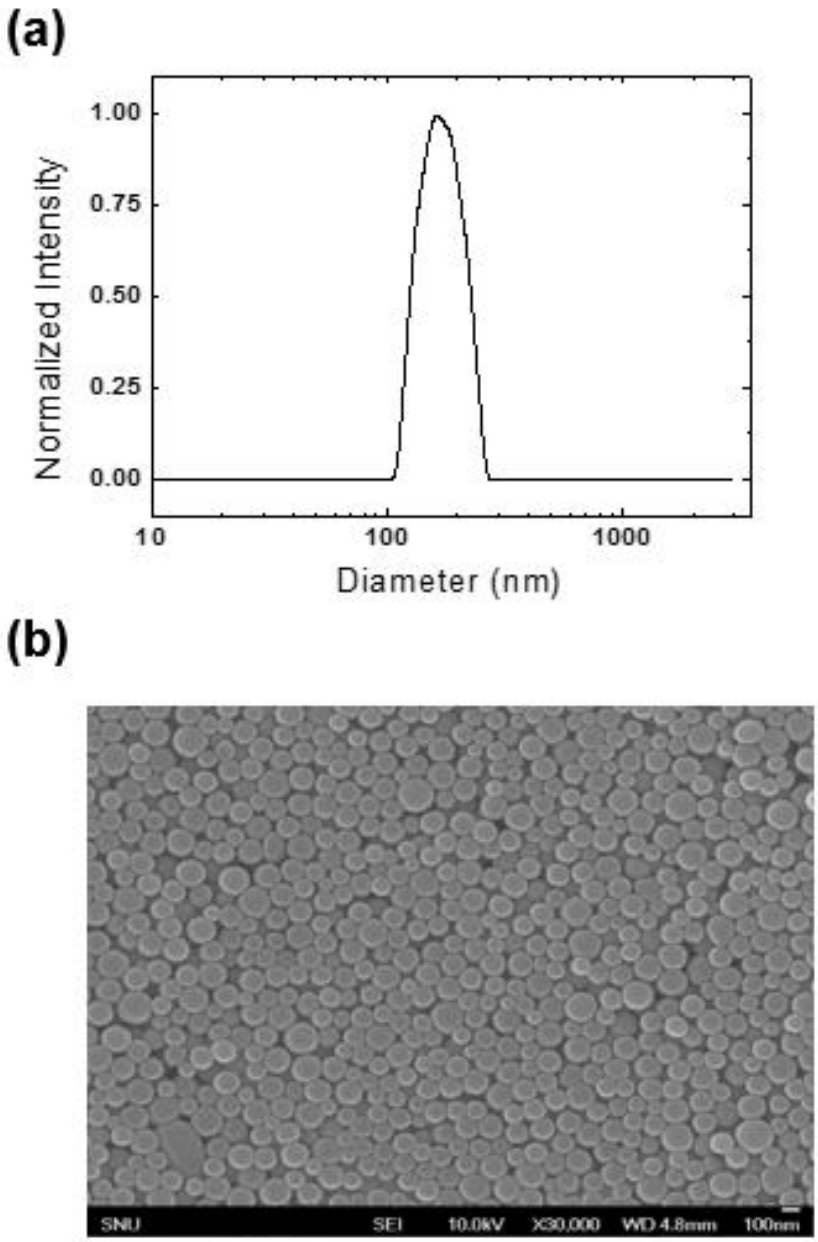

Figure 3. (a) DLS curve of polysulfide polymer NPs from trisulfide and TCP with CTAB. Average size is 202.2 ± 69.6 nm. (b) SEM images of polysulfide polymers obtained with CTAB.

2. Size Control of Sulfur-Rich Particles

In this interfacial polycondensation reaction between polysulfide and TCP, we could control the polysulfide nanoparticles size by changing the concentration of CTAB, the rank of polysulfide, and the chain length of the surfactant.

In Figure 4, the polymer particle size increased according to the CTAB concentration from 10×10^{-3} M to 100×10^{-3} M, nanoparticles size varying from 98×10^{-3} nm to 320×10^{-3} nm. Under concentration of CTAB of 10×10^{-3} M, ill-defined nanoparticles formed above which well-defined polymer nanoparticles started to form. Below critical concentration of CTAB (10×10^{-3} M), concentration of free phase transfer catalyst as well as surfactant does not exist enough which leads to formation of ill-defined nanoparticles and prolonged reaction time. From 10×10^{-3}M to 60×10^{-3} M, nanoparticles size increased steadily along with the CTAB concentration. CTAB can serve role as both free phase transfer catalyst and surfactant, resulting in well-defined polymer nanoparticles with narrow size distribution. While, slight increase is shown above 60×10^{-3} M. This phenomenon can be explained by correlation of concentration of free phase transfer catalyst and surfactant concentration. As polysulfide polymer

nanoparticles formation proceed, the amount of cationic surfactant at the surface of nanoparticles increase, which leads to decrease of free phase transfer catalyst.

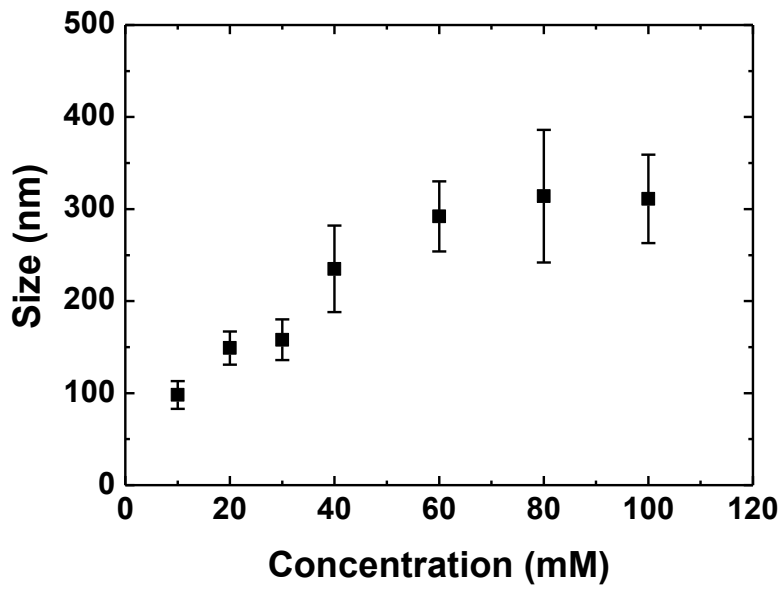

Figure 4. Size distribution of polysulfide polymer NPs from trisulfide and various concentration of CTAB. The average size and standard deviation was measured from SEM images of more than 100 NPs per sample.

Rank of polysulfide, the average number of sulfur atoms in sodium polysulfide, could be controlled by the ratio of elemental sulfur (S_8) and sodium sulfide (Na_2S) in the synthesis of sodium polysulfide according to the equation below:

$$\mathbf{Na_2S + \frac{x-1}{8} S_8 \rightarrow Na_2S_x}$$

Where x in the equation is called rank of polysulfide. We could control the ratio between sodium sulfide/elemental sulfur from 10 mmol/ 2.5 mmol for rank 2 to 10 mmol/ 4.375 mmol for rank 4.5 polysulfide. As rank of polysulfide increased, the size of monomer (polysulfide) increased along with the rank thus expected to be possible to control the resulting polymer nanoparticles. Figure 5 shows that size of nanoparticles increase along with the polysulfide rank from 2 to 4.5, which suggests a method for direct control of polymer nanoparticle size by changing of polysulfide rank.

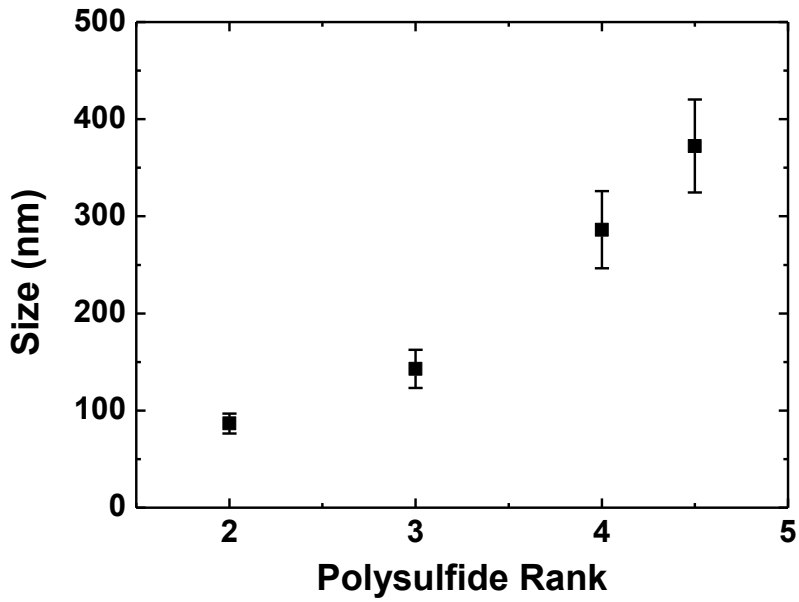

Figure 5. Size distribution of polysulfide NPs depending on polysulfide rank in the presence of CTAB.

In Figure 6, nanoparticles obtained from different rank of polysulfide are shown. From disulfide polymer to tetrasulfide polymer nanoparticles, increase of size was detected. Further analysis of DLS (Figure 7, 8, 9) shows narrow DLS curve.

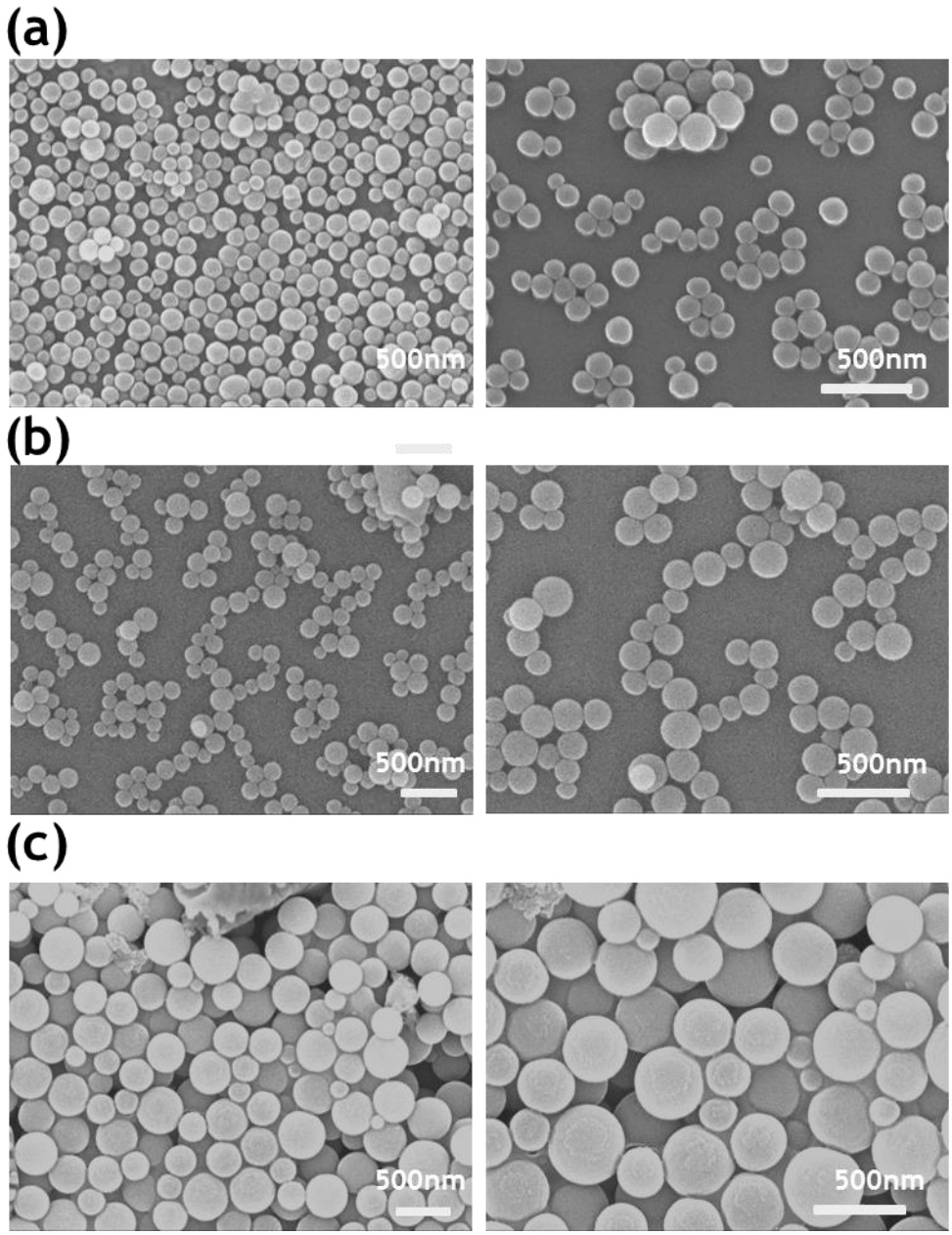

Figure 6. SEM images of NPs obtained from TCP and (a) disulfide, (b) trisulfide, (c) tetrasulfide in the presence of CTAB.

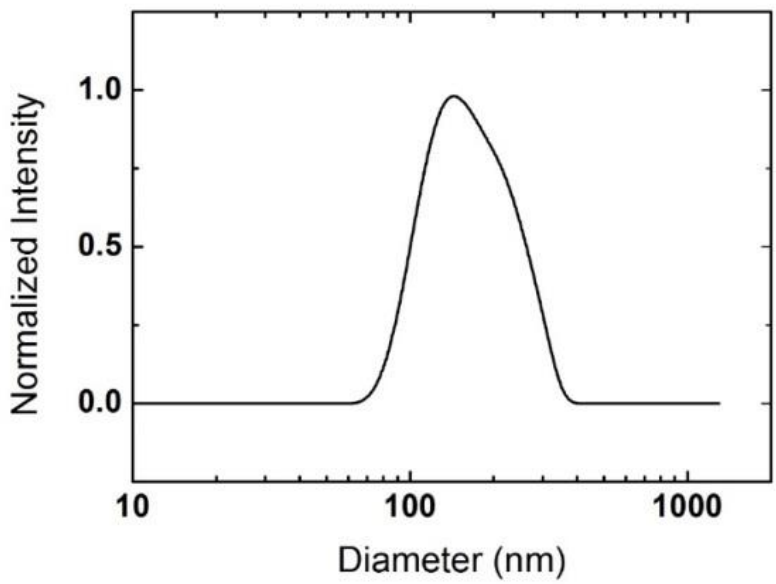

Figure 7. DLS curve of polysulfide polymer NPs from disulfide and TCP with CTAB. Average size is 169.9 ± 55.8 nm.

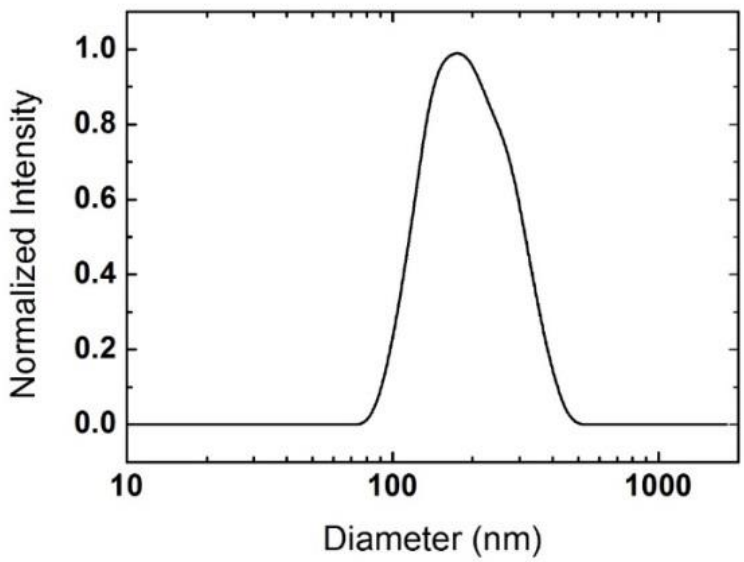

Figure 8. DLS curve of polysulfide polymer NPs from trisulfide and TCP with CTAB. Average size is 202.2 ± 69.6 nm.

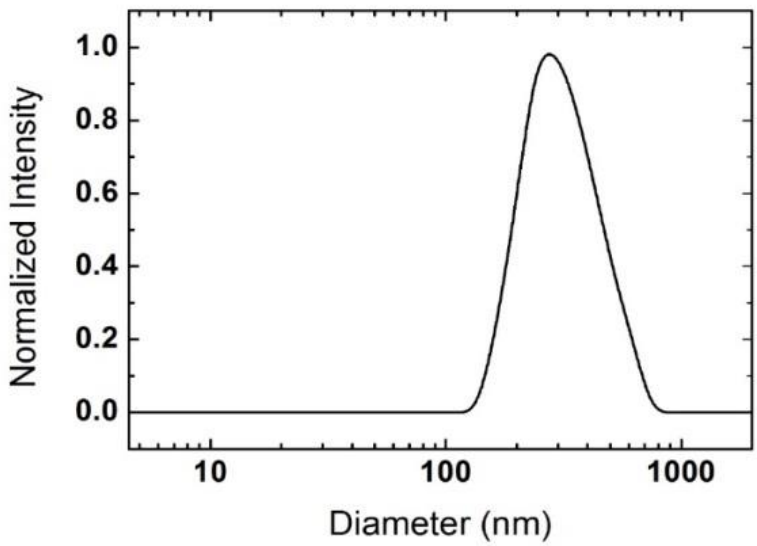

Figure 9. DLS curve of polysulfide polymer NPs from tetrasulfide and TCP with CTAB. Average size is 323.0 ± 112.1 nm.

In addition to the size control of nanoparticles, sulfur content could be controlled in the same way. With variation of sulfur content of the polysulfide monomers, resulting polymer nanoparticles' content also varied (Table 1). By calculating sulfur content from EA data, the resulting polymers had consistent sulfur content with the rank of starting polysulfide.

Rank	C (%)	H (%)	S (%)
2	26.89	3.78	68.78
3	20.68	2.90	76.33
4	16.68	2.32	80.89
4.5	14.25	1.97	83.73

Table 1. Elemental analysis of NPs from various rank of polysulfide and TCP in the presence of CTAB.

Carbon chain length of surfactant also change the size of nanoparticles. The polymer particle size decreases according to the surfactant chain length from 14 (TTAB) to 18 (OTAB),

nanoparticles size varying from 499.0×10^{-3} nm to 303.6×10^{-3} nm. (Figure 10). As carbon chain length increases, critical micelle concentration decreases, resulting in formation of nanoparticle in smaller size. (Figure 11) Nanoparticles are also synthesized well like in the previous cases and SEM images shows well-defined spherical shaped nanoparticles. (Figure 12)

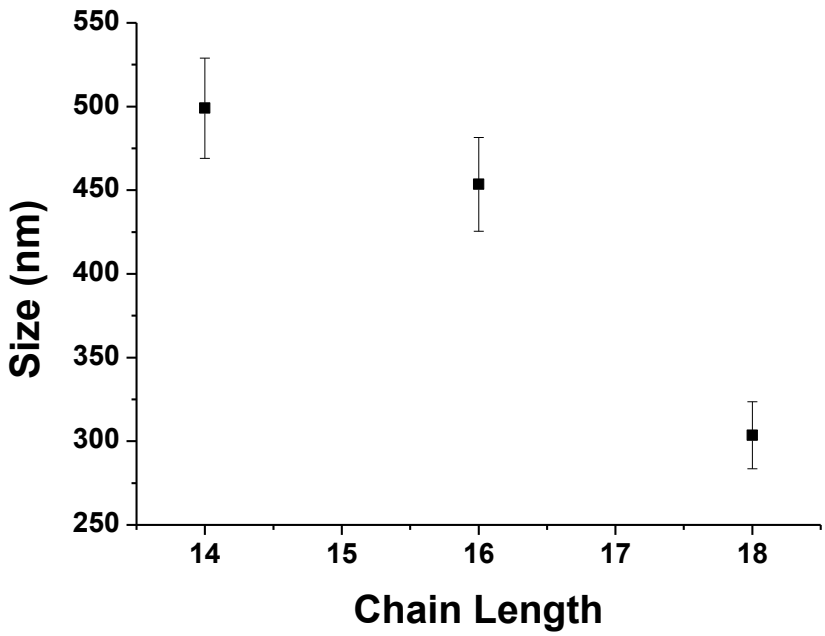

Figure 10. Size distribution of polysulfide NPs depending on the chain length of surfactant.

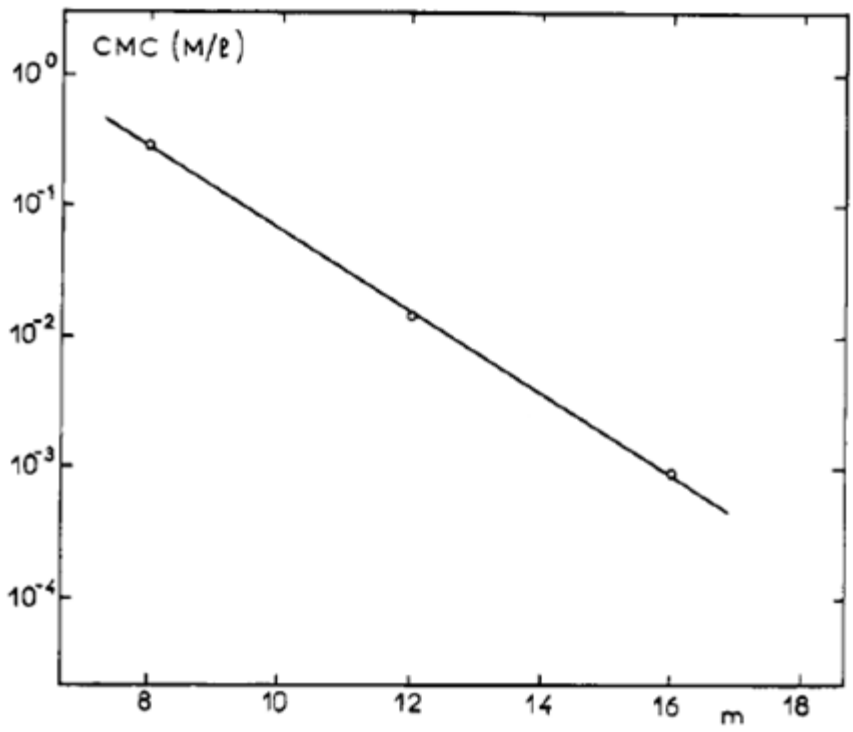

Figure 11. Variation of the cmc with the number of carbon atoms (m) in the alkyl chain of $C_mH_{2m+1}N^+(CH_3)_3Br^-$ surfactant at 25℃.

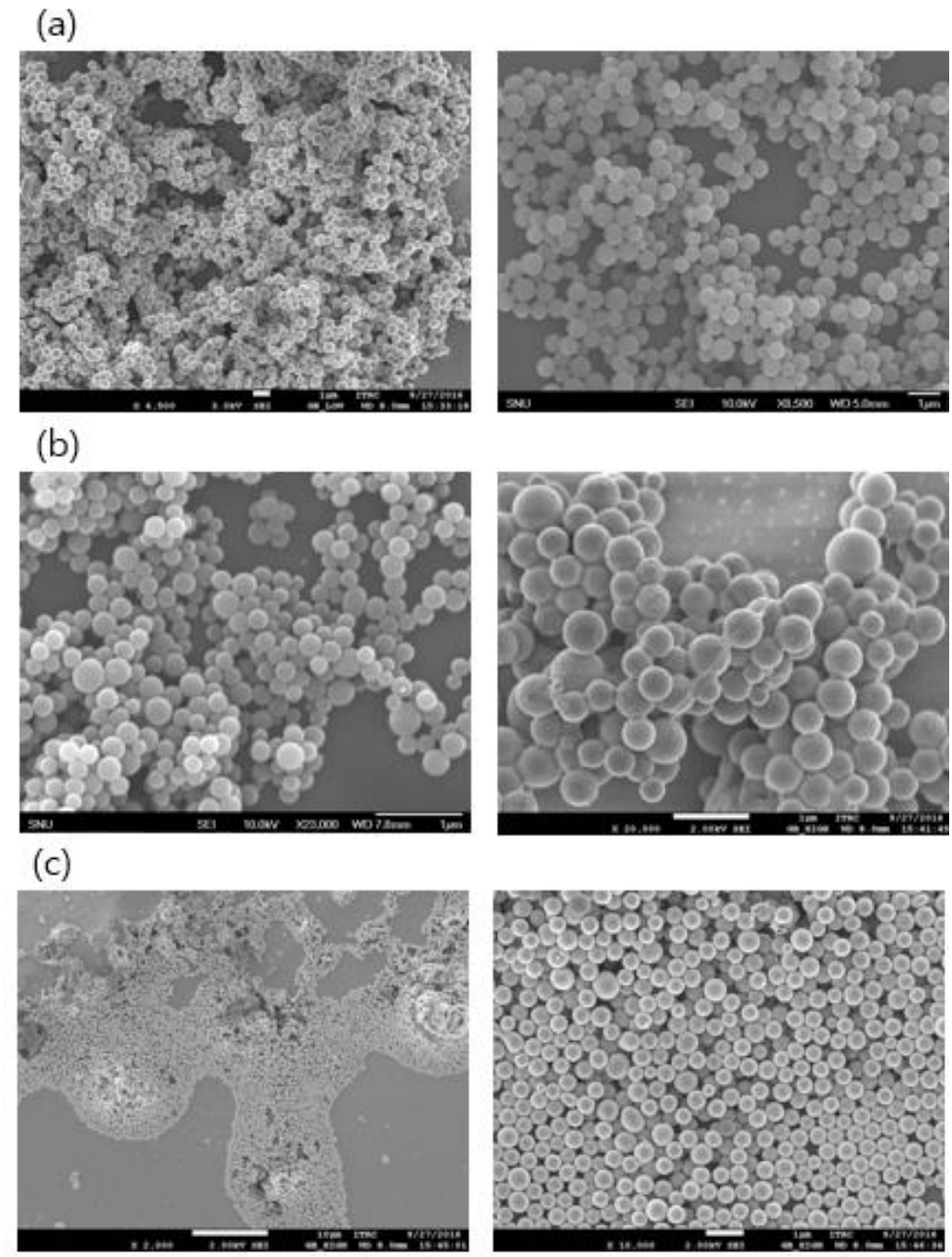

Figure 12. SEM images of NPs obtained from TCP and (a) TTAB, (b) CTAB, (c) OTAB in the presence of Tetra-n-butylammonium bromide (TBAB).

3. Proposed Mechanism for Sulfur-Rich NP Formation

Three kinds of surfactants were treated with polysulfide and TCP for polycondensation. Triton x-100 (non-ionic), SDS (anionic) and CTAB (cationic) are used with sodium trisulfide and TCP to yield turbid white dispersion.

For Triton x-100, morphology is not spherical but irregular cubic-like shape. And for SDS, spherical particles are shown but very sparsely and their size is not uniform. Unlike nonionic and anionic surfactant, CTAB could serve dual role as a surfactant and PTC to promote interfacial polycondensation between polysulfide anion and organic TCP. Synthesized nanoparticles have spherical shape and narrow size distribution. (Figure 13)

This critical change on both the morphology and the reaction time depending on the charge of surfactant used is attributed to the role of cationic surfactant during interfacial polycondensation. Only in case of cationic surfactant, transfer of polysulfide in aqueous phase to TCP in organic phase could be supported. Therefore, cationic charge of CTAB could promote the interaction with anionic polysulfide (Figure 5) to carry into the organic phase, which leads to reduction of reaction time and regular morphology in spherical shape. (Figure 14)

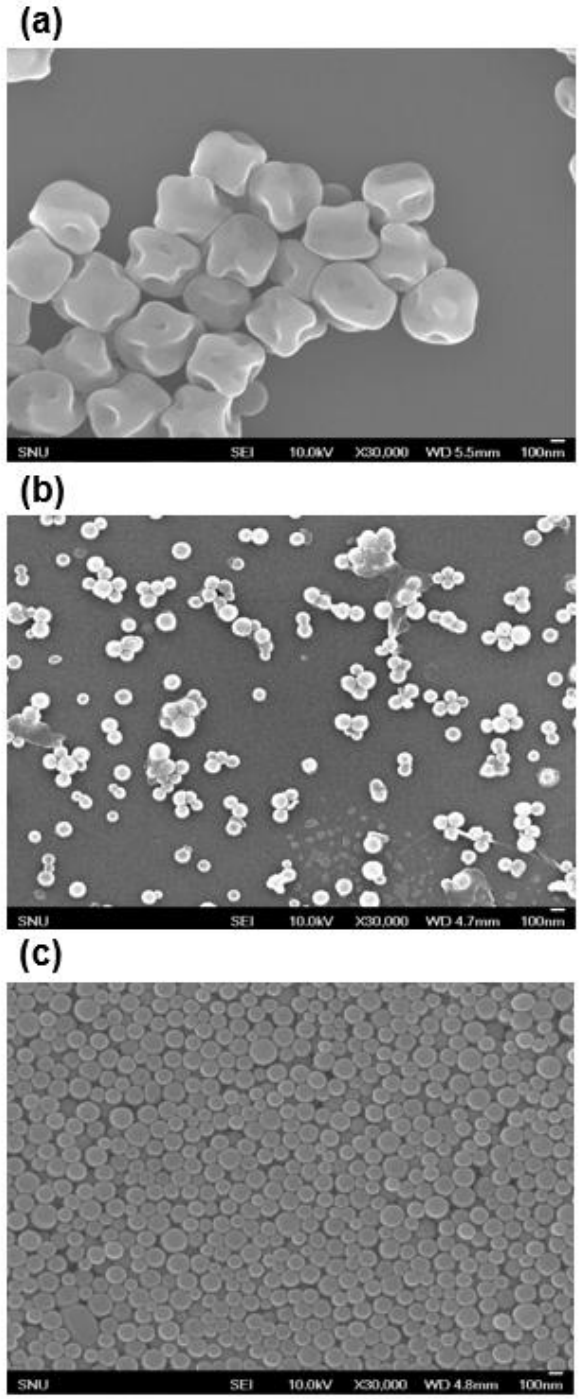

Figure 13. SEM images of polysulfide polymers obtained (a) with Triton X-100, (b) with SDS, (c) with CTAB.

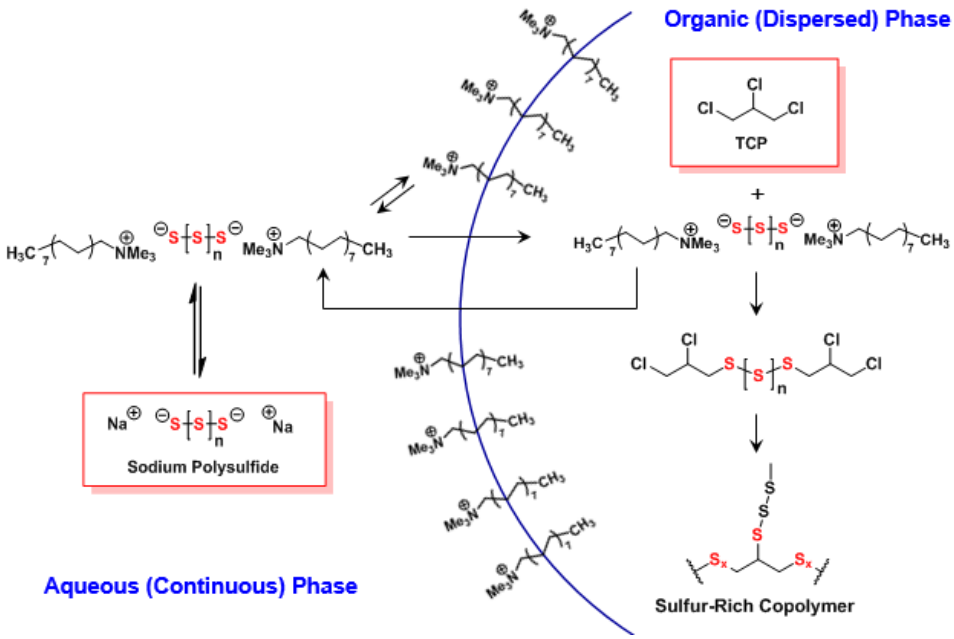

Figure 14. Schematic illustration of dual role of cationic CTAB during formation of polysulfide polymer NPs.

To prove this suggested mechanism, additional experiment is carried out. Instead of CTAB, which has dual role of surfactant and PTC, TBAB (act as a PTC) and non-ionic surfactant are used. Figure 15 shows schematic synthesis procedure of this experiment.

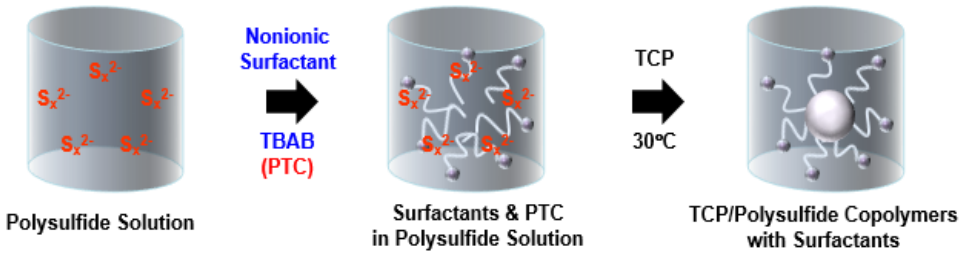

Figure 15. Synthetic procedure of polysulfide polymer from sodium trisulfide and 1,2,3-trichloropropane (TCP) in the presence of non-ionic surfactant, and phase transfer catalyst.

When using non-ionic surfactant like Triton X-100, Brij S20, and Brij C10, spherical shaped nanoparticles are synthesized well as is the case for CTAB, and it could be shown in SEM images (Figure 16). Following these results, suggested mechanism that cationic surfactant do dual role of transferring aqueous anionic polysulfide to organic phase TCP and stabilizing micelle as a surfactant could be proved indirectly.

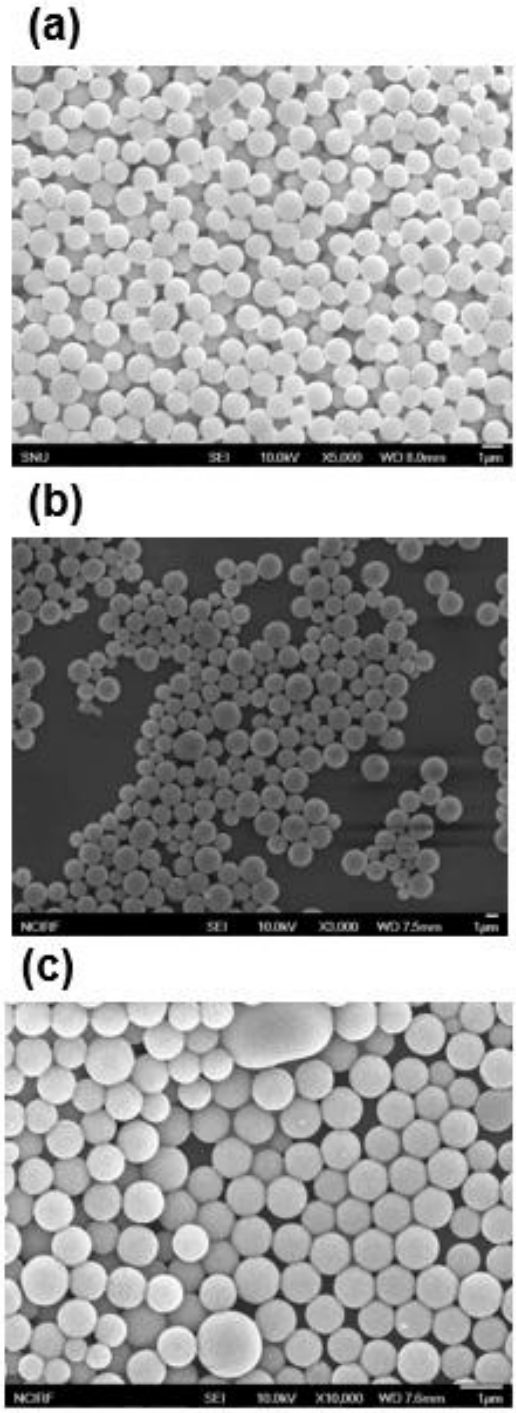

Figure 16. SEM images of polysulfide polymers obtained (a) with Triton X-100, (b) with Brij S20, (c) with Brij C10.

4. Surface Modification of Sulfur-Rich NPs

One major hurdle to utilize sulfur nanoparticle is aggregation after washing with water. Surfactants on surface of nanoparticles are easily washed out during purification step and surface positive charge disappeared to cause aggregation of nanoparticles. According to EA analysis of nanoparticles, after washing, no nitrogen is detected, suggesting that all cationic surfactants containing nitrogen are eliminated (Table 2). In addition, zeta potential of reaction mixtures was measured to be positive (+42.2 mV) before washing with water but negative (−21.3 mV) after washing due to the elimination of cationic surfactant localized on the surface of polymer nanoparticles. (Figure 17)

	S(%)	C(%)	H(%)	N(%)	Total(%)
Reaction mixture	72.2	22.7	3.3	1.5	99.7
After washing with water	75.5	21.2	2.1	0	98.8

Table 2. Elemental analysis of polysulfide polymer NPs from trisulfide and TCP as reaction mixture with CTAB and after washing with water.

Figure 17. Elimination of positive charge on the surface of nanoparticles after washing with water.

To solve this problem, we use the thiol−ene click reaction between new surfactants containing terminal vinyl moieties and sulfur radical induced by UV. It is well known that dynamic covalent bonding of sulfur−sulfur bond could be formed under UV radiation at which cleavage of sulfur bond occurs to produce radicals.

New surfactants, containing terminal olefin, could be synthesized from commercially available ω−pentadecalatone. It takes radical addition reaction with sulfur radical, making covalent bond on the surface of nanoparticles, which have tolerance for washing with water. This method allows for the preparation of stable dispersion of polysulfide nanoparticles with positively charged surfaces.

To confirm the surface modification through covalent bond, zeta potential before/after washing the mixture of PTAB and tetrasulfide polymer nanoparticles was measured. Measured zeta potential according to reaction time. Data shows that above 10min, zeta potential almost fully recovered as initial value (Figure 18). The resulted nanoparticles are expected to have positive charge on their surface via covalent bond with PTAB.

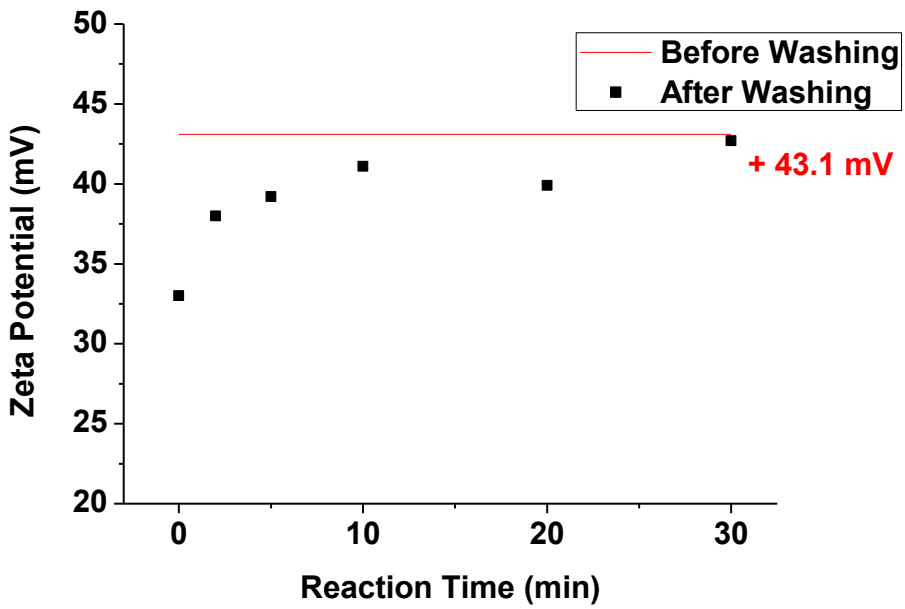

Figure 18. Zeta potential measurements of surface-modified NPs by PTAB before/after washing.

Ⅳ. Conclusion

Sulfur-rich polymer nanoparticles were synthesized in water through the interfacial polycondensation of sodium polysulfide and TCP in dilute condition with cationic surfactant. In addition, size of the particles could be easily controlled by rank of polysulfide, concentration of surfactant, and chain length of surfactant. In this system, CTAB serves dual role as a surfactant and phase transfer catalyst, suggesting new synthesis mechanism. It could be proved indirectly by experiment separating the dual role of CTAB into non-ionic surfactant and Phase transfer catalyst individually.

The CTAB could be easily removed after polycondensation by centrifugation-redispersion with water. Resulting polymer nanoparticles readily aggregate due to decrease of positive zeta potential of surface. Using thiol-ene click reaction between surfactant containing terminal olefin and sulfur radical under UV radiation, washing-tolerant covalent bond could be made.

The nanoparticles with cationic charge on the surface are probable to be exploited for insoluble polymer-supported phase transfer catalyst.

References

1. J. Lim, J. Pyun and K. Char, *Angew. Chem. Int. Ed.,* 2015, **54**, 3249-3258.

2. United States, Bureau of Mines and Geological Survey (U.S.), Mineral commodity summaries, Report 0160-5151, U.S. Dept. of the Interior, Bureau of Mines, Washington, D.C., 2009.

3. S. Kim, R. Kubec and R. A. Musah, *J. Ethnopharmacol.*, 2006, **104**, 188-192.

4. Z. Liang, G. Zheng, W. Li, Z. W. Seh, H. Yao, K. Yan, D. Kong and Y. Cui, *ACS Nano,* 2014, **8**, 5249-5256.

5. B. Dunn, H. Kamath and J. M. Tarascon, *Science*, 2011, **334**, 928-935.

6. K. Nakabayashi, T. Imai, M.-C. Fu, S. Ando, T. Higashihara and M. Ueda, *J. Mater. Chem. C.*, 2015, **3**, 7081-7087.

7. J. J. Griebel, S. Namnabat, E. T. Kim, R. Himmelhuber, D. H. Moronta, W. J. Chung, A. G. Simmonds, K. J. Kim, J. van der Laan, N. A. Nguyen, E. L. Dereniak, M. E. Mackay, K. Char, R. S. Glass, R. A. Norwood and J. Pyun, *Adv. Mater.,* 2014, **26**, 3014 -3018.

8. Raymond F. Bacon and Rocco Fanelli, *J. Am. Chem. Soc.,* 1943, **65**, 639-648.

9. A. V. Tobolsky and A. Eisenberg, *J. Am. Chem. Soc.,* 1959, **81**, 780-782.

10. R. H. Arntson, F.W. Dickson and G. Tunell, *Science*, 1958, **128**, 716 - 718.

11. R. Steudel, *Top. Curr. Chem.,* 2003, **231**, 127 - 152.

1991, **267**, 57-62: P. Zhang, L. Wu, Z. Bu, and B. -Geng, *J. Appl. Polym. Sci.*, 2008, **108**, 3586-3592.

12. H. Lucke, ALIPS, Hüthig & Wepf, 1992 / 1994.

13. M. R. Kalaee, M. H. N. Famili and H. Mahdavi, *Macromol. Symp.* 2009, **277**, 81-86.

14. M. R. Kalaee, M. H. N. Famili, H. Mahdavi and A. Naderi, *Polymer Science, Ser. B.*, 2010, **52**, 286-291.

15. W. Podkoscielny and W. Kowalewska, *J. Polym. Sci., Part A: Polym. Chem.*, 1984, **22**, 1579-1586.

16. M. Makosza, *Pure Appl. Chem.*, 1975, **43**, 439-462.

17. S. Sundarrajan and K. S. V. Srinivasan, *Macromol. Rapid Commun.*, 2004, **25**, 1406-1409.

18. S. Sundarrajan, M. Surianarayanan and K. S. V. Srinivasan, *J. Polym. Sci.,* 2005, **43**, 638-649.

19. Y.-T. Chern and B.-S. Wu, *J. Appl. Polym. Sci.*, 1996, **61**, 1853-1863.

20. K. H. Kim, J. Y. Moon, D. H. Ha and D. W. Park, *Catal. Lett.,* 2002, **75**, 385-395.

21. H. Mahdavi, E. Haghani and B. Malakian, *React. Funct. Polym.*, 2006, **66**, 1033-1040.

22. M. R. Kalaee, M. H. N. Famili, H. Mahdavi, *Polym.-Plast. Technol. Eng.*, 2009, **48**, 627 - 632.

23. Y. Kobayashi, M. Nakano, G. B. Kumar and Kishihara, *J. Org. Chem.*, 1998, **63**, 7505-7515.

24. J. P. Rao and K. E. Geckeler, *Prog. Polym. Sci.,* 2011, **36**,

25. a) C. Charcosset and H. Fessi, *J. Membrane Sci.*, 2005, **266**, 115-131; b) C. Charcosset , H. Fessi, *Rev. Chem. Eng.*, 2005, **21**,1-32; c) T. Yanagishita, R. Fujimura, K. Nishio , H. Masuda , Langmuir, 2010, **26** , 1516-1519.

26. K. Bouchemal, S. Briancon, E. Perrier, H. Fessi, I. Bonnet and N. Zydowicz, *Int. J. Pharm.,* 2004 , **269** , 89-100.

27. R. Zana, M. Benrraous, and R. Rueff, *Langmuir.*, 1991, **7**, 1072-1075

28. Jeewoo Lim, Unho Jung, Won Tae Joe, Eui Tae Kim, Jeffrey Pyun, Kookheon Char, *Macromol Rapid Commun.*, 2015, **36**, 1103-1107

29. Unho Jung, *서울 : 서울대학교 대학원*, 2016

국문 초록

박 정 민(Jeongmin Park)

화학생물공학부

(School of Chemical & Biological Engineering)

The Graduate School

Seoul National University

전 세계적으로 에너지 사용량이 급증함에 따라, 석유와 천연 가스 정제의 부산물로 인한 황의 생성량이 많아지고 있다. 황은 높은 전기화학적 용량, 높은 굴절률과 같은 여러가지 장점이 있고 이에따라 싸고 많은 양의 황을 응용하는 방안에 대해 많은 관심이 쏠리고 있다. 이러한 응용 가능성에 있어 한가지 가장 큰 문제점은 황이 일반적인 용매에 대해 용해도가 매우 낮다는 점이다. 따라서, 황의 다양한 장점들을 충분히 이용하기 위해서는 가공 가능한 형태의 고 – 황 함량 물질을 만드는 방법을 찾는 것이 중요하다.

여기서 우리는 소듐 설파이드와 1,2,3-트라이클로로프로페인을 물에서 계면 고분자 중합을 시켜 만든 고-황 함량 고분자 나노 입자의 합성 메커니즘과 표면개질을 소개한다. 세가지 종류 (음이온, 중성, 양이온) 의 계면활성제 중에, 오직 양이온 계면활성제의 경우에만 구형의 잘

형성된 나노 입자를 얻음을 알 수 있다. 이것은 양이온 계면활성제만이 음이온의 폴리설파이드 이온을 마이셀 안으로 이동시키는 상태 전이 촉매의 역할을 할 수 있기 때문이다. 중성 계면활성제와 상태 전이 촉매를 사용하여 황 나노 입자를 합성함으로써 이러한 메커니즘을 간접적으로 증명할 수 있다.

고-황 함량 나노 입자는 사슬 끝이 변형된 계면활성제와, 라디칼을 생성하는 자외선 처리의 방법으로 표면 개질이 가능하다. 이러한 방법으로 안정적으로 양전하를 띄어 분산이 잘되는 나노 입자를 얻을 수 있다.

Keywords: 황, 폴리설파이드 고분자, 표면 고분자 중합, 고분자 나노 입자, 메커니즘, 상태 전이 촉매, 표면 개질

student number : 2015-21065